
Article:
Sirvent, P., Garrido, M.Á., Sharp, J. et al. (2 more authors) (2020) Improving the oscillating wear response of cold sprayed Ti-6Al-4V coatings through a heat treatment. Surface and Coatings Technology, 399. 126128. ISSN 0257-8972

https://doi.org/10.1016/j.surfcoat.2020.126128

Improving the oscillating wear response of cold sprayed Ti-6Al-4V coatings through a heat treatment

Paloma Sirvent[a,1,*], Miguel Ángel Garrido[a], Joanne Sharp[b], William Mark Rainforth[b], Pedro Poza[a]

[a] DIMME – Durability and Mechanical Integrity of Structural Materials, Escuela Superior de Ciencias Experimentales y Tecnología, Universidad Rey Juan Carlos, C/Tulipán s/n, 28933 Móstoles, Madrid, Spain

[b] Department of Materials Science and Engineering, University of Sheffield, Sir Robert Hadfield Building, Mappin St, Sheffield, S1 3JD, UK

* Corresponding author: paloma.sirvent@ietcc.csic.es

Abstract

Cold spray (CS) coating technique is being studied as a potential solution for repairing aircraft Ti-6Al-4V components. This work is focused on the restoration of damaged components due to wear induced by vibrations. It is known that Ti-6Al-4V CS deposition shows difficulties to obtain non-porous coatings due to the high strength of this material, that is detrimental for wear resistance. In this sense, performing a post-heat treatment leads to lower porosity CS Ti-6Al-4V coatings and improves their mechanical properties, and thus, a better tribological behaviour is also expected. Therefore, the objective of this study was to determine the effect of a post-heat treatment on the wear resistance of Ti-6Al-4V coatings deposited by the CS technique. Ti-6Al-4V CS coatings were used, which have been sprayed with nitrogen as process gas at a temperature of 1100 °C and a pressure of 50 bar. The coatings were subjected to a solution heat treatment followed by a precipitation heat treatment. Oscillating and unidirectional sliding wear experiments were conducted on the coatings at room temperature and at 450 °C. A pin on disc configuration was used with a bearing steel counterbody. The

[1] Institute of Construction Science Eduardo Torroja – CSIC, c/ Serrano Galvache, 4, 28033 Madrid, Spain

results were compared to those obtained on the substrate (which represents the material to be repaired) and on the as-sprayed coating, which were derived from a previous work. The heat treated coating presented improved wear behaviour as compared to the substrate as well as to the as-sprayed coating, particularly during the high temperature tests. Wear at high temperature was dominated by material transference from the counterbody to the Ti-6Al-4V coating.

Keywords: Ti-6Al-4V titanium alloy; Cold Spray; Coating; Heat treatment; Tribology

1. Introduction

The cold spray (CS) technique is a thermal spray method for the deposition of coatings where particles of the material to be deposited are heated at temperatures lower than its melting point and accelerated by means of a carrier gas reaching supersonic velocities. The particles impact on the substrate getting the joint between them through a process of plastic deformation. The microstructure of the particles is retained in the deposited coating because the spraying temperatures are lower than the melting point of the sprayed material. In addition, the temperature gradients between the substrate and the coating and between the successive layers of deposited material are limited, so that the residual stresses are also restricted. All these features result in coatings with low porosity, controlled microstructure and high thicknesses [1]. This last property makes this spraying technique an ideal alternative to repair damaged components. This possibility becomes especially important in those components with high added value and high cost.

Titanium alloys, as lightweight structural materials, are of interest for applications at room and moderately elevated temperature environments. For that reason, several applications of titanium alloys are focused on the aeronautical and medical industry. Specifically, the Ti-6Al-4V alloy is the most widely used titanium alloy due to its good machinability and excellent mechanical properties and corrosion resistance. Elements of aircraft engines (discs, blades, shafts and casings), or parts of the airframes (fasteners, landing gear trucks, large wing beams) are made of Ti-6Al-4V [2], [3]. During the life cycle of the aircraft, these elements will be subjected to continuous damage processes because of mechanical stresses, vibrations, and corrosion. The response of this alloy to mechanical and corrosion requirements has been extensively studied [4], [5]. Additionally, the damage induced by vibration, i.e. wear by fretting, has been also reported in previous works [6].

These damage processes, which are revealed during the life of the aircraft, require maintenance works that usually involve the replacement of the component when the damage is higher than a threshold value. Due to the high cost of these Ti-6Al-4V alloy components, their replacement with a new one highly increases the maintenance costs. In an attempt to reduce these maintenance costs, the repair of damaged surfaces through the deposition of Ti-6Al-4V coatings is presented as an alternative capable of achieving this objective.

The methods for Ti coating deposition can be classified in two categories. These are techniques where the feedstock powder is heated at temperatures above its melting point, and other techniques where the deposition temperature is lower than the melting point of the material. The first category includes conventional techniques like HVOF [7], laser cladding [8] or plasma spraying [9]. CS is the only technique which is included in the second category.

Coatings deposited by the techniques of the first category are characterized by high temperature gradients. The microstructure of the coatings is different from that of the sprayed particles and the residual stresses are significant. Consequently, the coatings have different properties from those of the particles used in the deposition process and the coatings thickness is limited. Therefore, CS deposition has clear advantages over the techniques included in the first category from the repairing point of view [10]. However, a coating deposition technique is a reliable repairing technique when the coatings generated on the damaged area have similar properties to those of the bulk material. Because of that, it is necessary to study the mechanical properties, the corrosion behaviour and the wear resistance of the coatings deposited by CS. Previous works have reported results concerning the wear resistance of Ti-6Al-4V coatings deposited by CS. In this sense, there are still few works related to the wear resistance of CS Ti-6Al-4V coatings because of their relatively recent development. Furthermore, as wear processes are influenced by a number of conditions and parameters within the system of study, there is a need of a larger investigation about the wear behaviour of these coatings. Besides that, the studies to date have shown interesting results. For

example, Khun et al. [11] deposited Ti coatings onto Ti-6Al-4V substrates by CS and they showed that the wear behaviour of the CS Ti coatings was improved compared to the bulk alloy. Additionally, to the authors knowledge, the oscillating wear in CS Ti-6Al-4V coatings has only been reported in studies conducted by the authors [12], [13]. The authors have studied the wear resistance of Ti-6Al-4V coatings deposited by CS on substrates of the similar Ti alloy [12]. Two different spraying temperatures were selected: 800 °C and 1100 °C. Oscillating and unidirectional sliding wear tests were conducted on the CS Ti-6Al-4V coatings against a bearing steel counterbody at room temperature (RT) and 450°C. The work concluded that the coating sprayed at 800 °C showed a poor wear resistance compared to the bulk material. However, the coating deposited at 1100 °C exhibited comparable or even better wear resistance to that of the substrate under oscillating movement. The porosity analysis reported values of 18% and 4% for the Ti-6Al-4V coatings deposited at 800 °C and 1100 °C, respectively. Then, it seems that, the lower the porosity of the coating, the better the wear resistance. Following this reasoning, it is worth asking whether the wear resistance of the coatings deposited at 1100 °C could be improved by increasing the cohesion strength of the coating, for example performing a heat treatment.

Sometimes, CS coatings show intersplat boundaries which are not metallurgically bonded. The non-bonded interfaces may act as crack nuclei under tensile loading. This deficiency could be alleviated by appropriate post heat treatments to induce recovery and recrystallization. The heat treatment at elevated temperatures could increase both tensile strength and ductility due to the increase in the metallurgically bonded area between the deposited particles. Wong et al. [14] studied the effect of the heat treatment of the resulting coatings on the mechanical properties of CS Ti-6Al-4V alloy. Nitrogen gas was used during the coating deposition process and the propellant gas temperature and pressure values were selected to maximize the particle impact velocity. The coatings were annealed at 600 and 800

°C. They observed through micro tensile tests an increase in the cohesion strength of the coatings treated at the highest temperature.

Moreover, Vo et al. [15], studied the effect of different heat treatments onto CS Ti-6Al-4V coatings deposited on Ti-6Al-4V substrates. Nitrogen and helium were used as propellant gases for the coatings deposition, working at a pressure of 4 MPa, and at 800 and 350 °C temperatures, respectively. Post-spray processing consisted of annealing the specimens in an argon atmosphere at different times and temperatures that ranged from 200 °C to 1025 °C. Among all of the heat treated (HT) nitrogen-sprayed coatings, they reported that those annealed at 1000 °C showed the larger increase in tensile strength. Thus, this result indicated that the increase in annealing temperature provides coatings with high metallurgical bonding. Besides, a study by Molak et al. [16] also reported good results after heat treating Ti-6Al-4V coatings deposited by warm spray thermal technique. They sprayed coatings at different pressures, from 1 to 4 MPa, and controlling the temperature of the propellant gas by diluting the combustion flame with nitrogen. Additionally, they conducted three different heat treatments that are recommended for Ti-6Al-4V in order to study their effect on the mechanical properties of the CS coatings [17]. They conducted a mill annealing, where the Ti-6Al-4V coatings were first heated at 750 °C for 1 h and subsequently cooled to RT. Recrystallization annealing was also performed, where the coatings were heated at 940 °C for 4 h, then furnace cooled to 760 °C at a rate of 1 °C/min, further cooled to 480 °C at a rate about 5 °C/min in the furnace, and finally cooled outside the furnace to RT. In addition, a beta annealing was done, where coatings were first heated at 1025 °C for 1 h and then cooled to RT at a rate higher than 85 °C/min. Finally, a subsequent annealing was performed at 760 °C for 2 h and followed by a cooling outside the furnace. After the mill annealing, they observed a significant decrease in microhardness. However, the samples treated by recrystallization and beta annealing showed a noticeable increase in microhardness. Additionally, they obtained that the tensile strength and the Young's modulus for all the heat-treated samples were

enhanced regarding to the as-received materials. These results are in agreement with those previously obtained by other researchers [18], [19].

Consequently, it seems that performing a post-heat treatment improves the mechanical properties of Ti-6Al-4V coatings deposited by CS. Several relationships between mechanical properties of materials and wear behaviour have been reported [20]. One of the most widely used is the Archard model [21], where a relationship between hardness and wear rate is established. This model predicts an increase in wear resistance of the material when so does its hardness. Therefore, a better tribological behaviour is expected when post-heat treatments are carried out on Ti-6Al-4V coatings deposited by CS.

Thus, the objective of this work has been to determine the effect of a post-heat treatment on the wear resistance of Ti-6Al-4V coatings deposited by the CS technique. This work is a further study from our previous study on the CS Ti-6Al-4V coatings wear behaviour under oscillating conditions [12].The wear resistance investigation of the same coating with a subsequent heat treatment is done here. The results of this work could provide a way to improve the behaviour of the CS Ti-6Al-4V coatings, from the tribological point of view, extending the useful life of the cold spray repaired components.

2. Materials

The materials studied in this investigation were CS Ti-6Al-4V coatings deposited on Ti-6Al-4V substrates with a following heat treatment. The microstructure, mechanical and tribological behaviour of the as-sprayed coating have been reported in our previous works [12], [22] and thus, the experimental procedure for the coatings deposition has already been detailed there. A gas atomized Ti-6Al-4V powder (supplied by LPW (United Kingdom)) was used for spraying. Table 1 shows the chemical composition of this powder. The particles presented a spherical morphology and a size of (-25+15) μm. This powder exhibits a martensitic α'-Ti microstructure [22]. The substrates were commercial Ti-6Al-4V plates

which presented an equiaxed and lamellar microstructure of α-Ti grains with β-Ti phase at the grain boundaries. The substrate was prepared before spraying by grinding with 120 grit. The coatings were sprayed with a commercial CGT Kinetiks 4000 series CS system using the deposition parameters reported in Table **1** Chemical composition of the Ti-6Al-4V used for the cold spray deposition [22].

Ti6Al4V Powder

Element (wt. %)									
Ti	**C**	**O**	**N**	**H**	**Fe**	**Al**	**V**	**Other (each)**	**Other (total)**
Balance	0.01	0.16	0.02	0.002	0.2	6.5	3.9	<0.1	<0.4

Table 2. The as-sprayed coatings were deposited with a nitrogen gas pressure of 50 bar and a temperature of 1100 °C (Table 2).

After the spraying process, some coupons were heat-treated. A strengthening heat treatment was selected because it provides excellent strength properties combined with ductility [23], [24]. The choice of this heat treatment was based on the need of high strength materials for the aeronautical industry. The response of the solution treating and aging cycle is reported to increase the strength of α-β alloys, as the Ti-6Al-4V alloy. The treatment was done on the as-sprayed coating following a two-step process. Firstly, a solution heat treatment was performed at ~1000 °C for 1h in high vacuum (lower than 10^{-7} torr), with a heating rate of 10 °C/min and followed by argon quenching to RT. The second stage was a precipitation heat treatment, which was conducted at 537 °C for 4 h, heating with a rate of 10 °C/min and followed by furnace cool.

Table 3 presents the porosity, thickness and roughness of the as-sprayed and HT coatings, which have already been reported [22]. Porosity values that are referred in this work were calculated using ten micrographs at x20 magnifications from the transversal section of the coatings. The hardness and elastic modulus were measured in our previous study [22].The

measurements were conducted by nanoindentation on the polished surfaces of the materials. A hardness of 3.86 ± 0.33 GPa was obtained on the HT coating, which was slightly lower, but similar, to that of the as-sprayed coating, 3.94 ± 0.36 GPa [22]. Both hardness values were higher than the Ti-6Al-4V feedstock particles hardness which was 3.01 ± 0.40 GPa. The elastic modulus was higher in the HT coating (117.0 ± 4.9 GPa) than in the as-sprayed coating (107.2 ± 3.4 GPa) because of the changes in microstructure after the heat treatment [22].

3. Methods

3.1. Microstructural characterization of the coating

A microstructural characterization by scanning electron microscopy (SEM) of the HT sample has been previously reported by the authors [22]. This microstructural analysis is completed here with XRD analyses which were performed by means of a Philips PW3040/00 X'Pert MPD/MRD diffractometer using Cu (Kα) radiation with λ= 1.54 Å. The diffraction patterns were recorded with an angle from 10 to 115 °. The step of angle for recording was of 0.02 °. The WebPDF 4+ software was used for the analysis with the database of the International Centre Diffraction Data (ICDD).

3.2. Wear tests

The wear tests were conducted following the same methods and testing parameters as those reported in [12], [13]. The experiments were performed with a Wazau TRM1000 tribometer using two different tests configurations: one applying a unidirectional sliding movement and a second one with an oscillating movement. The first type of motion was selected as a reference for the tests, while the second one was selected to simulate the oscillating tangential movements occurring between aircraft components subjected to vibrations. The oscillating tests consisted on a slow rotation of the counterbody with a superimposed high frequency vibration, as described elsewhere [12]. This configuration was the most similar to the

oscillation motion that was allowed by the tribometer. Therefore, the unidirectional sliding tests were only defined by the sliding speed of the rotation, and, in the oscillating tests, the rotation was defined by the sliding speed, while the oscillations were defined by the amplitude and frequency of the oscillating cycles.

A 100Cr6 steel (760 ± 17 HV, R_a= 0.62 ± 0.07 μm) was used as the counterbody, which was cleaned with soap and acetone before the test. The choice of the 100Cr6 steel for the counterbody was based on the application under study. Titanium can be found in contact with this material in some aircraft parts subjected to vibrations, such as in landing gears. Pins with a surface section of 2.5 X 6 mm were obtained from the coating samples and they were cleaned by means of an ultrasound bath in acetone for 10 min before the tests. The pins were weighed before and after the tests to obtain the weight difference, Δm. This value was then used to calculate the wear rate (δm) as the ratio of the weight loss of the pins (Δm) by the test time (Δt):

$$\delta m = \Delta m / \Delta t \quad (1)$$

The coefficient of friction (COF) was also obtained during the tests. The experimental parameters were selected to recreate the more severe wear conditions that could be found in titanium aircraft components. The unidirectional sliding experiments were performed at RT and at 450 °C, both with a sliding velocity of 0.26 m/s and a normal pressure between the pin and the counterbody of 30 MPa. The tests were stopped when the wear depth reached the limit of 600 μm, because the coatings thickness was ~670 μm. The oscillating tests were also performed at RT and at 450 °C, being fixed the sliding velocity at 0.0026 m/s, the normal pressure at 30 MPa, the oscillation amplitude at 596 μm and the oscillation frequency at 40 Hz. The test time in these experiments was limited by a maximum number of oscillating cycles of 100 000 as well as by the wear depth limit of 600 μm.

3.3. Wear mechanisms evaluation

The wear mechanisms evaluation was done through microstructural investigation by means of SEM using a Hitachi S3400N microscope. This analysis was conducted by the examination of the worn surfaces as well as the transverse section of the near surface of the pins after being cleaned within an alcohol ultrasound bath. The sliding direction is pointed out using black arrows in the micrographs showing worn surfaces in this manuscript. The cross sectional samples were metallographically prepared up to a final polishing of 0.04 μm (colloidal silica suspension, OP-U). Thus, the sliding direction corresponds to the perpendicular direction to the shown plane in all the cross-sectional images in this paper. Secondary electron (SE) and backscattered electron (BSE) micrographs were acquired. Energy dispersive X-ray microanalyses were also performed with a Bruker XFlash 5010 detector to examine possible variations in chemical composition at the contact surface.

Transmission electron microscopy (TEM) was also conducted in representative samples with a Jeol 2010F and a Jeol JEM -Z3100R05 microscopes. Bright field (BF) and dark field (DF) micrographs were acquired. EDX microanalyses, scanning transmission electron microscopy (STEM) and electron energy loss spectroscopy (EELS) and selected area electron diffraction patterns (SADPs) were also used for the study. The samples were prepared to examine the near surface at a transverse section to the sample surface. A FEI Helios Nanolab G3 UC focused ion beam (FIB/SEM) was used for the sample preparation.

The FIB specimens were prepared to analyse the perpendicular section of the near surface of the worn samples up to about 5 μm in depth. They were obtained by milling trenches around three sides of a previously deposited platinum strip (25×2.5×2.5 μm) on the sample surface. The milling was done using a beam current of 21 nA. Then, a micromanipulator needle was attached to the specimen surface to do the lift-out. The fourth side, by which the specimen was still attached to the sample, was milled and the specimen was lifted out. Finally, the sample was attached to a copper grid and it was conducted the final thinning of the specimen

using a decreasing current beam from 0.5 nA to 100 pA and an energy of 20 kV. The thinning was done down to a thickness < 100nm.

4. Results and discussion

4.1. Microstructural characterization of the coating

Figure 1 shows the XRD analyses conducted on the as-sprayed and on the HT coating. The main structural phase identified on the as-sprayed coating was the α-Ti phase (hexagonal closed packed (hcp), P63/mcm space group, a=b= 2.920 Å and c=4.700 Å). The structural phases formed on the surface of the HT coating were examined in its as-received state and after removing several microns by mechanical polishing (Figure 1). The XRD pattern from the coating in its as-received state revealed the formation of various structural phases on the most superficial surface. α-Ti structural phase was the main phase. Additionally, secondary phases were identified as TiO (face centred cubic (fcc), Fm-3m space group, a= 4.293 Å) and α_2-Ti phase (Ti_3Al, hcp, P63/mmc space group, a=b= 5.793 Å and c= 4.649 Å). The diffraction peaks obtained from the polished surface of the coating were indexed as α-Ti phase and β-Ti phase ($Ti_{0.7}V_{0.3}$, bcc, Im-3m space group, a= 3.211 Å). It was also observed that the XRD peaks were slightly broader in the as-sprayed coating diffractogram as compared to that of the HT coating. This result will be explained in the light of the SEM study.

Figure 2 shows the microstructure of the as-sprayed coating that has also been reported in a previous work [22]. The microstructure consisted of splats generated by the CS process as can be seen in Figure 2a. In addition, a martensitic microstructure was observed within the splats (Figure 2b). As the powder microstructure was also martensitic [22], this result indicated that the coating microstructure was not altered during the spraying.

Figure 3 presents a cross-section general view of the HT coating (Figure 3a) and higher magnification images of the etched cross section showing different areas of the coating: the top surface (Figure 3b), an intermediate area (Figure 3c), and the interface with the substrate (Figure 3d). This coating presented a porosity of 1.37 ± 0.62 % which was lower with regard to the as-sprayed coating (3.83 ± 0.39 %) (Table 3). Regarding the microstructure, SEM examination revealed that the characteristic splat structure of the as-sprayed coating (Figure 1b) had disappeared. The microstructure was formed by equiaxed grains surrounded by a secondary phase which corresponded to the α-Ti and β-Ti phases respectively. In addition, the cohesive strength of the as-sprayed and HT sample have been previously tested under tubular coating tensile (TCT) tests [25] following the developed method by HSU University [26]. The cohesive strength of the heat treated coating was ~1200 MPa, and it was significantly higher than that of the as-sprayed coating, ~350 MPa.

This fact means that the recrystallization and grain growth have occurred. This β-Ti phase, enriched in vanadium, precipitated in the intergranular areas (Figure 3c) and may promote a solid-state densification process during the post heat treatment, decreasing the porosity and favouring a metallurgical bonding between the deposited particles. This point was previously reported in other studies[27]–[30]. Consequently, this heat treatment has proven to be capable of generating a coating with improved cohesion regarding to as-sprayed one. Nay et al. [28] prepared Ti6Al4V coatings on commercial Ti-6Al-4V substrates by cold spray process. The coatings were heat treated in air at different temperatures, between 400 and1000 °C, for 6 h and then the oven was switched off to cool down the samples until RT. The effect of heat treatment temperature on the microstructure, mechanical and tribological properties was studied. They obtained that the diffusion between the sprayed Ti-6Al-4V particles was promoted when the heat treatment temperature was about 600 °C. Also, they reported recrystallization of the sprayed particles in the 800 °C HT samples, while grain growth was found in the microstructure of the 1000 °C HT coating. They concluded that a rapid cooling

from 1000 °C to RT would result in the formation of a martensitic phase in this coating. This effect was observed in the HT samples of the present study, as can be seen in Figure 3c. Some acicular grains were observed within the retain β-Ti grains, which probably consisted on martensitic α'-Ti. This result was associated to the argon quenching performed at the end of the first step in the heat treatment process. Rapid cooling and subsequent martensitic transformation can improve the performance of many titanium alloys [31]. However, because of the small lattice distortion of acicular martensitic structure in titanium alloy, the strengthening effect is slight [32]. The formation of this martensitic phase within the β-Ti grains explains the hardness values of the as-sprayed and HT coating. The as-sprayed coating hardness was shown to increase as regard to that of the powder due to the work hardening effect during the CS deposition as it was reported [22]. Thus, the recrystallization during the heat treatment was expected to lower the coatings hardness. As it was pointed, the HT coating presented a slightly lower value, but quite near to that of the coating before the treatment.

Moreover, the recrystallized α-Ti grains generated during the heat treatment also explain the finding related to the XRD peaks width. The as-prayed coating presented broader peaks due to the smaller grains in its microstructure. This coating was mainly constituted by martensitic grains, which consists on fine laths (Figure 2b). Conversely, the HT coating microstructure was mostly formed by recrystallized α-Ti grains.

A thin layer measuring 1.9 ± 0.6 μm was generated at the top surface of the coating (Figure 3b). This layer was related to the TiO phase which was detected by XRD analysis in the as-received sample, without polishing. In addition, the presence of retained β-phase was shown to be reduced at the upper region of the coating, below the above-mentioned layer. This feature is usually observed when oxygen diffusion occurs during Ti oxidation near the surface and it is known as α-case [24]. The reduction in β-phase is caused because oxygen is an α-stabilizing element.

The interface of the coating with the substrate was also modified with regard to the coating without HT (Figure 3d) [22]. A metallurgical bonding was generated by diffusion with no distinguishable interface line. The lower porosity, as well as the metallurgical bonding enhancement between the splats and at the interface with the substrate, were especially interesting characteristics for improving the CS coating wear resistance.

4.2. Wear tests

4.2.1. COF and wear rate results

Figure 4 shows the COF and the wear rate (δm) results of the wear experiments on the HT coating. The obtained results on the substrate and on the as-sprayed coating, that were reported in our previous work [12], have also been included to facilitate the comparison.

Regarding the HT coating, the COF and δm value were shown to be lower during the oscillating tests than those observed during the unidirectional sliding experiments (Figure 4). This result suggested the activation of different wear mechanisms between the two types of motion. On the one hand, during the oscillating tests in this coating, a COF of ~0.1 was obtained when testing at both RT and 450 °C temperatures. However, in spite of the similar COF values, the δm was different. The pin mass was increased after the test conducted on the HT coating under oscillating conditions at 450 °C. For this reason, the δm value of this test is not shown in the graph. This finding was related to a major contribution of counterbody material transfer to the pin under the mentioned testing conditions, and it will be further discussed later in the text. On the other hand, the unidirectional sliding experiments performed on the HT coating, showed different COF values when testing at RT and at 450 °C, being ~0.3 and ~0.45 respectively. The increase in COF at 450 °C for this coating was accompanied by a δm reduction from 0.027 to 0.006 mg/s.

Considering first the unidirectional sliding tests, the comparison of the obtained results in the HT coating with those observed in the substrate and in the as-sprayed coating, indicated that the COF and δm values presented similar trends (Figure 4). However, it should be noted that the wear resistance of the HT coating in the unidirectional sliding tests was improved with regard to the as-sprayed coating when testing at RT and with regard to the substrate and the as-sprayed coating when testing at 450 °C (Figure 4b). The wear resistance enhancement in RT tests was also observed by Khun et al. [28] as a consequence of heat treating a Ti-6Al-4V CS coating. They studied the effect of heat treatment temperature on microstructure and mechanical and tribological properties of cold sprayed Ti-6Al-4V coatings. After the spraying process, the coatings were HT at different temperatures of 400–1000 °C. The tribological properties of the coatings were measured against a 100Cr6 steel ball of 6 mm in diameter in a circular path of about 2 mm in diameter for about 189 m at a sliding speed of 3 cm/s under a normal load of 1 N. They obtained that the heat-treated coating at 1000 °C showed similar COF values to the as-deposited coating and that its specific wear rate was lower than that obtained on the as-deposited coating.

On the other hand, the trends observed during the oscillating tests differed between the materials (Figure 4). While the wear rates of the substrate and the as-sprayed coating were increased when increasing the testing temperature, the wear rate was decreased in the case of the HT coating (Figure 4b). Negative wear rates were even measured for these experiments in the HT coating. Therefore, while the as-sprayed coating presented an improved wear resistance with regard to the substrate during the RT tests, the HT coating has shown an enhancement of the wear resistance at 450 °C. These findings will be clarified by the microstructural investigation.

4.2.2. Wear mechanisms

The COF variability measured in these tests suggested that different wear mechanisms were being activated by the different testing conditions. Thus, the wear mechanisms have been analysed by means of the microstructural examination of the tested samples.

Figures 5a and b show the worn surface of the HT coating tested under unidirectional sliding conditions at RT, where abrasive grooves and debris particles were found. The debris was found as loose particles and generating agglomerates, which could measure several hundreds of microns in size. An example of these particle agglomerates is shown in the inserted image in Figure 5b, which was formed by a mixture of Ti-6Al-4V and counterbody particles as revealed by EDX microanalyses (Figure 5c). Counterbody particles were also found adhered to the surface. In addition, cracks were generated on the surface of the sample as a consequence of the high stresses occurring during the test. Moreover, the investigation of the cross section of the sample revealed that a mechanically mixed layer (MML) was generated (Figures 6a and b), which was similar to that formed under the same experimental conditions in the other materials [12]. The MML consisted on a mixture of Ti-6Al-4V alloy with traces of counterbody particles as revealed by EDX map microanalyses (Figure 6b). No oxides were found in the MML. The layer was developed discontinuously and with a variable thickness along the cross section. A maximum thickness of ~40 μm was measured along the studied cross section. Additionally, the MML microstructure includes debris agglomerates highly deformed in the sliding direction

The morphology of the worn surface of the HT coating after a unidirectional sliding test at 450 °C presented a smoother appearance as compared to the sample tested at RT, as can be seen in Figures 5d and e. EDX microanalysis revealed that oxides were formed on the surface. The surface appeared to be particularly oxidized at the sites where a higher content of Fe from the counterbody was present, as can be distinguished in the BSE micrographs and EDX microanalyses (Figures 5e and f). A continuous MML was observed at the top surface of a studied cross section of this sample (Figure 6c). The MML was around 20 μm thick and it was

extended up to 50 μm in some regions. A mixture of Fe oxides and Ti-6Al-4V formed the MML generating large layers parallel to the surface as can be seen in the EDX maps in Figure 6d, indicating high plastic deformation.

The presence of residual scratches on the worn surfaces (Figures 5a and c) combined with delamination processes, allowed identifying the abrasion and adhesion as the main wear mechanisms involved during the unidirectional sliding tests. Moreover, a high plastic deformation was shown to be promoted by the unidirectional sliding motion. Regarding the inclusion of Fe oxides in the MML, found during the 450 °C tests (Figures 6c and d), this result has let to identify the contribution of an oxidative wear during the high temperature tests.

In addition, the generated MMLs on the HT coating during the unidirectional sliding tests were shown to provide a slight improvement in wear resistance as compared to that in the as-sprayed coating (Figure 4b). This fact was mainly associated with the MML characteristics and it could also be related to the lower degree of porosity of the HT coating and to the enhanced interface with the substrate of this coating. Moreover, the lower δm observed in the HT coating could be also associated to the initial TiO layer generated on the surface, as will be discussed later. Furthermore, the HT coating δm was decreased when the testing temperature was increased (Figure 4b), as it has been observed in the substrate and in the as-sprayed coating [12]. This finding was related to the presence of oxides in the MML which were shown to provide a protective effect against wear. The presence of oxides has also been found before in the MML generated on substrate and as-sprayed coating samples tested under the same experimental conditions [12].

Figures 5g and h present micrographs of the worn surfaces generated after an oscillating test at RT on the HT coating. Abrasion grooves and debris particles (loose or agglomerated) dispersed on the surface were observed. Some debris particles presented a higher content of oxygen indicating the possible formation of Ti or Fe oxides during the process (EDX 1,

Figure 5i). The presence of transferred material from the counterbody was also observed on the surfaces (EDX 2, Figure 5i). The microstructural study by SEM of the RT oscillating test sample revealed the formation of an MML at the top surface of the sample (Figure 6e) which was discontinuously distributed along the cross section and presented a maximum thickness of ~8 μm. As can be seen in Figures 6e and f, delamination of the MML was found at some regions of the cross sectional cut. The MML consisted of a mixture of the Ti alloy of the coating with some traces of Fe rich phases from the counterbody as it is shown in the EDX maps presented in Figures 6e and f.

Comparing the MML of the unidirectional sliding and oscillating tests (Figures 6a and e), it can be observed that there was a higher plastic deformation in the generated MMLs during the unidirectional sliding tests (Figures 6a and c). Conversely, fragmented particles were observed on the worn samples after the oscillating tests (Figure 6e and g). It can thus be suggested that there was a third body action during the oscillating tests. This may justify the lower COF and δm values obtained in the oscillating tests regarding to the sliding ones (Figure 4).

A subsequent TEM investigation of the near surface region of this sample has shown that the microstructure of the MML was nanocrystalline. Figure 7 shows a TEM micrograph of the top surface of this sample. At the most superficial region of the sample, the grains presented small sizes with equiaxed morphologies. The DP acquired from that region consisted of a ring diffraction pattern indicating the formation of a nanostructured grain region. Below this nanostructured region, it can be seen that the grains were larger in size. These larger grains presented equiaxed morphologies as well as elongated shapes, oriented parallel to the surface, indicating that they could have been deformed. The composition of the grains was identified as the Ti-6Al-4V alloy by EDX analysis along the entire TEM sample. STEM EDX map analysis showed the presence of a secondary phase enriched in V, the β-Ti phase, which was

previously identified in the microstructural characterization of this sample. This phase was observed generating bands with different morphologies and its formation in the coating was associated with the heat treatment. A large band of this phase measuring several microns in length was observed in the FIB sample (not shown). But there were also observed smaller bands of the V rich phase at the top region of the sample, within the nanograin structure (Figure 8). These smaller traces appeared to be fractions from the β-Ti phase which might have been broken during the test. These results indicated that the MML had been created through the formation of transfer particles that are detached by adhesion and their following mechanical mixing [33], [34].

Regarding the worn sample after the 450 °C oscillating test (Figures 5j, k and l), a relatively large quantity of counterbody material was found adhered on its surface covering areas of hundreds of microns. This result indicated that the material transfer from the counterbody was important during the oscillating test performed at 450 °C in this coating. The MML, which was observed on the studied cross sectional cut of this sample, is presented in Figures 6g and h. In a similar way to the features observed in the plan view surface, a considerable layer of transferred material was created at the top surface of the sample. The layer was continuous, and its thickness was ~25 μm and at some regions it was extended up to ~36 μm. The EDX maps included in Figure 6h indicated that a thick layer of oxidized counterbody material was adhered to the coating's surface. On the other hand, as it can be seen in the figure, almost no wear of the coating was observed. Instead, a significant counterbody material was adhered to the surface. Moreover, it can be distinguished a thin layer of about 2 μm in thickness between the Ti-6Al-4V coating and the oxidized transferred material, which appeared to be constituted of Ti oxide which could be associated with the oscillating test conditions.

The MML that was observed by SEM was also analysed through the TEM study. Figure 9 shows a TEM sample of the near surface microstructure. In the figure, there could be

distinguished an MML generated at the upper region of the sample, which was constituted of small grains. The thickness of this layer measured ~0.6 μm. The chemical composition was identified as Fe, O and Cr and a smaller amount of Ti and Al elements as shown in the EDX microanalysis (Figure 9c). In the EELS spectrum of the MML which is reported in Figure 10, the shape of the O-K edges and Fe-$L_{2,3}$ edges appeared to be similar to the ones associated to the FeO or Fe_3O_4 [35]. On the other hand, the α-Ti matrix of the coating was identified under the oxide layer. The formation of this MML is therefore related to an adhesive wear process in which the counterbody material is transferred to the pin. This result was not expected, because the counterbody material was originally harder than the pin. In addition, the oxidized state of the transferred material also suggested that the oxidation wear mechanism was also involved in the process. It should be noted that the studied FIB sample did not show the 2 μm TiO layer that was identified by SEM. This implies the TiO layer was not continuous between the coating and the transfer layer, and the FIB sample was obtained from a region of the worn surface in which this TiO layer was absent, possibly due to wear.

The most surprising result to emerge from the HT coating wear study was that the wear process of the system at 450 °C under oscillating motion was opposite to the expected and to that observed in the as-sprayed coating, as it was pointed above. Since the counterbody material was harder than the coating, it was expected that the coating should have been more abraded by the counterbody asperities rather than the opposite [36]. However, the coating appeared marginally worn and the MML, which was found on the surface of the pin, was primarily based on counterbody material. This result was also deduced from the negative weight differences obtained from the weight measurements of the pins before and after the tests. The pins were shown to increase in weight, and this fact could only be explained if material from the counterbody was adhered to the pin's surface. A possible explanation for this result may be related to an external TiO layer which could be generated during the oscillating wear tests. Waterhouse et al. [37] reported that Ti alloys develop oxides at 600 °C

that are thin, very protective and not disrupted by the fretting action. Matikas et al. [38] predicted temperature variations near the fretting path for Ti alloys in the 800 to 1000 °C region. Alyabev [39], however, reported temperatures above 400 °C near the fretting path. Consequently, in the oscillating tests carried out in this work, temperatures of 600 °C (to take an average of the two reported values) could be reached in the contact, justifying the formation of the TiO layer. This protective layer may have had a decisive role in the wear rate, limiting the wear of the Ti alloy and promoting the wear of the counterbody. This oxide layer was probably harder than the oxidized counterbody. In fact, the EDX maps (Figure 6h) of a worn sample have indicated that this layer had remained unworn in some regions of the sample. Previous studies on Ti [40], [41] or Ti-6Al-4V [42], [43] wear behavior have reported an enhancement in wear resistance when the samples were oxidized because the oxidized samples presented higher hardness. For example, TiO_2 presents a hardness value in the range of 1000 to 1500 HV [44], which is significantly higher than the untreated Ti. The oxidation of the counterbody was also considered because some iron oxides, as the Fe_3O_4 (450 to 550 HV) or FeO (250 to 350 HV) [45], are softer than the steel alloy used for the experiments (760 HV). However, this effect was not observed in the tests conducted in the as-sprayed coating or in the substrate. Therefore, the findings point to a possible influence of the TiO layer which resulted harder than the Fe oxides. Moreover, the MML did not show the deformed layers generated during the unidirectional sliding experiments. Some particle fragmentation was observed instead in the MML (Figure 6g). It is therefore likely that a third body wear was also occurring during the oscillating tests at 450 °C.

Therefore, the wear process in oscillating tests at RT and 450 °C was mainly produced by a third body action. This justifies that in both cases the COF was similar (Figure 4a). However, in the case of RT tests, the wear process may be mainly produced in the coating, while at 450 °C it seems that this process may occur on the counterbody. This could explain the differences observed in the coatings wear rates (Figure 4b).

Finally, it should be noted that the differences found between the COF and δm values of the unidirectional sliding and the oscillating tests seemed to be caused by a higher plastic deformation generated by the unidirectional sliding motion. The samples tested under unidirectional sliding motion have shown features, as greater cracks on the surfaces and thicker MMLs with clear plastic deformation signs that were not observed after the oscillating tests. As could be observed in Figure 6, it seems that the wear process involves delamination of the surfaces in contact. Some of this debris was retained in the contact between the surfaces forming the MML. Therefore, it seems that the behaviour of the tribological system could be conditioned by the morphology and deformation capacity of the MML. The MML has a morphology characterized by high deformation (Figures 6a and c). However, in the oscillating tests, this MML showed a different morphology. It did not show a high plastic deformation (Figures 6e and g). The wear process appeared to be more dominated by a third body action what led to a reduction in COF and wear rates (Figure 4). Therefore, the differences observed in the morphology and composition of the MML could explain the differences between the unidirectional sliding and the oscillating tests in the wear resistance (Figure 4b).

5. Conclusions

The aim of this investigation was to evaluate the wear response under oscillating motion of Ti-6Al-4V CS coatings sprayed at a process gas temperature of 1100 °C and a pressure of 50 bar with a following heat treatment. Oscillating wear experiments were performed at two different testing temperatures: RT and 450 °C. Unidirectional sliding experiments were also conducted at similar experimental conditions as a reference. The results of this study indicate that:

- The HT Ti-6Al-4V CS coating has shown an enhanced wear resistance as compared to the as-sprayed coating and the bulk material under high temperature environment (450 °C). This result was associated to the microstructure of the samples. The

microstructure of the HT coating presented a lower porosity and enhanced interfaces between the splats and at the interface with the substrate with regard to the as-sprayed coating. In addition, a TiO layer was generated during the HT which was shown to provide wear protection particularly testing under oscillating high temperature environment.

- A higher plastic deformation was shown to be promoted during the unidirectional sliding experiments, while wear in the oscillating tests seemed to be more dominated by a third body action. These mechanisms variability between both types of motion experiments led to lower COF and wear rates in the Ti-6Al-4V coatings tested under the oscillating conditions.
- The wear mechanisms during the unidirectional sliding experiments at RT were a combination of abrasion and adhesion. Moreover, the high plastic deformation induced by the mode of motion led to the formation of highly deformed debris layers in the MML. The same wear mechanisms plus oxidative wear were observed when testing at 450 °C. The activation of the oxidative wear led to a COF increment and a lower wear rate in the process.
- Regarding the oscillating tests, the wear mechanisms at RT were also abrasion and adhesion. The MML presented in this case less signs of plastic deformation, the debris particles seemed to be fragmented instead. During the 450 °C experiments, oxidative wear was activated and it led to a higher wear in the counterbody material than in the coating.

6. Acknowledgements

This work has received funding from the European Union's Seventh Framework Programme under grant agreement ACS3-GA-2013-605207 (CORSAIR). The authors would also like to thank the financial support from the Spanish government CICYT under grants MAT2013-

41784-R (REMACOLDS) and MAT2016-76928-C2-2-R (DURESPRAY) and from Rey Juan Carlos University for the grant to conduct a research visit.

Declarations of interests: None

References:

[1] V. K. Champagne, *The Cold Spray Materials Deposition Process: Fundamentals and Applications*, 1st ed. Woodhead Publishing, 2007.

[2] M. Peters, J. Kumpfert, C. H. Ward, and C. Leyens, "Titanium alloys for aerospace applications," *Adv. Eng. Mater.*, vol. 5, no. 6, pp. 419–427, 2003, doi: 10.1002/adem.200310095.

[3] R. R. Boyer, "An overview on the use of titanium in the aerospace industry," *Mater. Sci. Eng. A*, vol. 213, no. 1–2, pp. 103–114, 1996, doi: 10.1016/0921-5093(96)10233-1.

[4] H. Yu *et al.*, "Mechanical properties and microstructure of a Ti-6Al-4V alloy subjected to cold rolling, asymmetric rolling and asymmetric cryorolling," *Mater. Sci. Eng. A*, vol. 710, pp. 10–16, Jan. 2018, doi: 10.1016/J.MSEA.2017.10.075.

[5] S. Carquigny, J. Takadoum, and S. Ivanescu, "Corrosion and tribocorrosion study of 316L steel, Ti–6Al–4V and Ti–10Zr–10Nb–5Ta," *Tribol. - Mater. Surfaces Interfaces*, vol. 13, no. 2, pp. 112–119, 2019, doi: 10.1080/17515831.2019.1596625.

[6] S. Basseville, D. Missoum-Benziane, and G. Cailletaud, "3D finite element study of the fatigue damage of Ti--6Al--4V in presence of fretting wear," *Comput. Mech.*, vol. 64, no. 3, pp. 663–683, Sep. 2019, doi: 10.1007/s00466-019-01675-6.

[7] M. Oksa, E. Turunen, T. Suhonen, T. Varis, and S.-P. Hannula, "Optimization and Characterization of High Velocity Oxy-fuel Sprayed Coatings: Techniques, Materials, and Applications," *Coatings*, vol. 1, no. 1, pp. 17–52, 2011, doi: 10.3390/coatings1010017.

[8] J. Mazumder, "Laser-aided direct metal deposition of metals and alloys," *Laser Addit. Manuf.*, pp. 21–53, Jan. 2017, doi: 10.1016/B978-0-08-100433-3.00001-4.

[9] K. Jayaraj and A. Pius, "Biocompatible coatings for metallic biomaterials," *Fundam. Biomater. Met.*, pp. 323–354, Jan. 2018, doi: 10.1016/B978-0-08-102205-4.00016-7.

[10] M. F. Smith, "Comparing cold spray with thermal spray coating technologies," *Cold Spray Mater. Depos. Process*, pp. 43–61, Jan. 2007, doi: 10.1533/9781845693787.1.43.

[11] N. W. Khun, A. W. Y. Tan, W. Sun, and E. Liu, "Wear and Corrosion Resistance of Thick Ti-6Al-4V Coating Deposited on Ti-6Al-4V Substrate via High-Pressure Cold Spray," *J. Therm. Spray Technol.*, vol. 26, pp. 1393–1407, 2017, doi: 10.1007/s11666-017-0588-8.

[12] P. Sirvent, M. A. Garrido, S. Lozano-Perez, and P. Poza, "Oscillating and unidirectional sliding wear behaviour of cold sprayed Ti-6Al-4V coating on Ti-6Al-4V substrate," *Surf. Coatings Technol.*, vol. 382, p. 125152, Jan. 2020, doi: 10.1016/j.surfcoat.2019.125152.

[13] P. Poza *et al.*, "Oscillating Contact Wear in Cold Sprayed Ti6Al4V Coatings for Aeronautical Repairs," *Mater. Sci. Forum*, vol. 941, pp. 1686–1691, Dec. 2018, doi: 10.4028/www.scientific.net/MSF.941.1686.

[14] W. Wong, E. Irissou, J. G. Legoux, P. Vo, and S. Yue, “Powder Processing and Coating Heat Treatment on Cold Sprayed Ti-6Al-4V Alloy,” *Mater. Sci. Forum*, vol. 706, pp. 258–263, 2012, doi: 10.4028/www.scientific.net/MSF.706-709.258.

[15] P. Vo, E. Irissou, J. G. Legoux, and S. Yue, “Mechanical and microstructural characterization of cold-sprayed Ti-6Al-4V after heat treatment,” *J. Therm. Spray Technol.*, vol. 22, no. 6, pp. 954–964, 2013, doi: 10.1007/s11666-013-9945-4.

[16] R. M. Molak, H. Araki, M. Watanabe, H. Katanoda, N. Ohno, and S. Kuroda, “Effects of Spray Parameters and Post-spray Heat Treatment on Microstructure and Mechanical Properties of Warm-Sprayed Ti-6Al-4V Coatings,” *J. Therm. Spray Technol.*, vol. 26, no. 4, pp. 627–647, 2017, doi: 10.1007/s11666-016-0494-5.

[17] *ASM Handbook, Metals Handbook, Vol.4 Heat Treating*, 9th ed. Materials Park, OH, USA: ASM International, 1981.

[18] R. E. Blose, B. H. Walker, R. M. Walker, and S. H. Froes, “New opportunities to use cold spray process for applying additive features to titanium alloys,” *Met. Powder Rep.*, vol. 61, no. 9, pp. 30–37, 2006, doi: 10.1016/S0026-0657(06)70713-5.

[19] W. Wong *et al.*, “Cold Spray Forming of Inconel 718,” *J. Therm. Spray Technol.*, vol. 22, no. 2, pp. 413–421, Mar. 2013, doi: 10.1007/s11666-012-9827-1.

[20] K. Kato and K. Adachi, “Wear Mechanisms,” in *Modern Tribology Handbook. Vol 1: Principles of Tribology*, 1st ed., B. Bhushan, Ed. Boca Raton, Florida: CRC Press, 2001, p. 28.

[21] J. F. Archard, “Contact and Rubbing of Flat Surfaces,” *J. Appl. Phys.*, vol. 24, no. 981, 1953.

[22] M. A. Garrido, P. Sirvent, and P. Poza, “Evaluation of mechanical properties of Ti6Al4V cold sprayed coatings,” *Surf. Eng.*, vol. 34, no. 5, pp. 399–405, 2017, doi: 10.1080/02670844.2017.1398442.

[23] F. F. Schmidt and R. A. Wood, “Heat Treatment of Titanium and Titanium Alloys,” *Nasa Tech. Memo.*, 1966.

[24] M. J. Donachie, *Titanium: A Technical Guide*, 2nd ed. ASM International, 2000.

[25] P. Sirvent, “Analysis of the Cold Spray method for maintenance andoverhaul of aeronautical Ti components,” Rey JuanCarlos University, 2018.

[26] T. Schmidt, F. Gärtner, H. Assadi, and H. Kreye, “Development of a generalized parameter window for cold spray deposition,” *Acta Mater.*, vol. 54, no. 3, pp. 729–742, 2006, doi: 10.1016/j.actamat.2005.10.005.

[27] C. Li, W. Li, and H. Liao, “Examination of the Critical Velocity for Deposition of Particles in Cold Spraying,” *J. Therm. Spray Technol.*, vol. 15, no. 2, pp. 212–222, 2006, doi: 10.1361/105996306X108093.

[28] N. W. Khun, A. W. Y. Tan, W. Sun, and E. Liu, “Effect of Heat Treatment Temperature on Microstructure and Mechanical and Tribological Properties of Cold Sprayed Ti-6Al-4V Coatings,” *Tribol. Trans.*, 2016, doi: 10.1080/10402004.2016.1244584.

[29] H. Y. Lee, S. H. Jung, S. Y. Lee, and K. H. Ko, “Fabrication of cold sprayed Al-intermetallic compounds coatings by post annealing,” *Mater. Sci. Eng. A*, vol. 433, no. 1–2, pp. 139–143, 2006, doi: 10.1016/j.msea.2006.06.044.

[30] T. Stoltenhoff, C. Borchers, F. Gärtner, and H. Kreye, “Microstructures and key properties of cold-sprayed and thermally sprayed copper coatings,” *Surf. Coatings Technol.*, vol. 200, pp. 4947–4960, Apr. 2006, doi: 10.1016/j.surfcoat.2005.05.011.

[31] S. Sundaresan and G. D. J. Ram, “Use of magnetic arc oscillation for grain refinement of gas tungsten arc welds in α–β titanium alloys,” *Sci. Technol. Weld. Join.*, vol. 4, no. 3, pp. 151–160, Jun. 1999, doi: 10.1179/136217199101537699.

[32] W. Wang and C. Han, “Microstructure and wear resistance of Ti6Al4V coating fabricated by electro-spark deposition,” *Metals (Basel).*, vol. 9, no. 1, 2019, doi: 10.3390/met9010023.

[33] D. A. Rigney, L. H. Chen, M. G. S. Naylor, and A. R. Rosenfield, “Wear processes in sliding systems,” *Wear*, vol. 100, no. 1–3, pp. 195–219, 1984, doi: 10.1016/0043-1648(84)90013-9.

[34] I. Hutchings and P. Shipway, *Tribology: Friction and Wear of Engineering Materials*, 2nd ed. Oxford: Elsevier Ltd, 2017.

[35] C. C. Calvert, A. Brown, and R. Brydson, “Determination of the local chemistry of iron in inorganic and organic materials,” *J. Electron Spectros. Relat. Phenomena*, vol. 143, no. 2-3 SPEC. ISS., pp. 173–187, 2005, doi: 10.1016/j.elspec.2004.03.012.

[36] I. Hutchings, *Tribology: Friction and Wear of Engineering Materials*, 1st ed. Butterworth-Heinemann, 1992.

[37] R. B. Waterhouse and A. Iwabuchi, “High temperature fretting wear of four titanium alloys,” *Wear*, vol. 106, no. 1–3, pp. 303–313, Nov. 1985, doi: 10.1016/0043-1648(85)90114-0.

[38] T. E. Matikas and P. D. Nicolaou, “Prediction of contact temperature distribution during fretting fatigue in titanium alloys,” *Tribol. Trans.*, vol. 52, no. 3, pp. 346–353, 2009, doi: 10.1080/10402000802563117.

[39] A. Y. Alyab’ev, Y. A. Kazimirchik, and V. P. Onoprienko, “Determination of temperature in the zone of fretting corrosion,” *Sov. Mater. Sci.*, vol. 6, no. 3, pp. 284–286, 1973.

[40] K. Aniołek, M. Kupka, A. Barylski, and G. Dercz, “Mechanical and tribological properties of oxide layers obtained on titanium in the thermal oxidation process,” *Appl. Surf. Sci.*, vol. 357, pp. 1419–1426, 2015, doi: 10.1016/j.apsusc.2015.09.245.

[41] K. Aniołek, M. Kupka, and A. Barylski, “Sliding wear resistance of oxide layers formed on a titanium surface during thermal oxidation,” *Wear*, vol. 356–357, pp. 23–29, 2016, doi: 10.1016/j.wear.2016.03.007.

[42] H. Guleryuz and H. Cimenoglu, “Surface modification of a Ti-6Al-4V alloy by thermal oxidation,” *Surf. Coatings Technol.*, vol. 192, no. 2–3, pp. 164–170, 2005, doi: 10.1016/j.surfcoat.2004.05.018.

[43] A. Biswas and J. Dutta Majumdar, “Surface characterization and mechanical property evaluation of thermally oxidized Ti-6Al-4V,” *Mater. Charact.*, vol. 60, no. 6, pp. 513–518, 2009, doi: 10.1016/j.matchar.2008.12.014.

[44] J. G. Heinrich and F. Aldinger, Eds., “Ceramic coating with solid lubricant ability for engine applications,” in *Ceramic Materials and Components for Engines*, John Wiley & Sons, 2008, p. 678.

[45] L. E. Samuels, “Surface oxidation, decarburization and carburizing,” in *Light Microscopy of Carbon Steels*, ASM International, 1999, p. 502.

Table 1 Chemical composition of the Ti-6Al-4V used for the cold spray deposition [22].

Ti6Al4V Powder									
Element (wt. %)									
Ti	**C**	**O**	**N**	**H**	**Fe**	**Al**	**V**	**Other (each)**	**Other (total)**
Balance	0.01	0.16	0.02	0.002	0.2	6.5	3.9	<0.1	<0.4

Table 2 CS process parameters for the coatings deposition [22].

CS parameters	
Substrate surface preparation	Ground (120 grit)
Process Gas	Nitrogen
Process Gas Temperature	1100 °C
Process Gas Pressure	50 bar
Spraying distance	50 mm
Traverse speed	500 mm/s
Number of Passes	4
Track spacing	1 mm
Spraying angle	90º
Powder feeder wheel rotational speed	3 rpm
Nozzle type	SiC, water-cooled

Table 3 Porosity, thickness and roughness (R_a, arithmetical mean roughness) of the Ti-6Al-4V CS coating before (as-sprayed) and after being heat treated (HT coating) [22].

	Porosity (%)	**Thickness (µm)**	**R_a (µm)**
As-sprayed coating	3.83 ± 0.39	684 ± 27	7.92 ± 0.32
HT coating	1.27 ± 0.62	677 ± 25	8.11 ± 0.30

List of figure captions:

Figure 1 XRD patterns acquired from the surface of the as-sprayed CS coating and from the as-received and the polished surface of the HT Ti-6Al-4V coating.

Figure 2 a) SE image showing the etched cross section of the as-sprayed coating and b) a higher magnification image from the up-right area on (a) showing a detail of the martensitic microstructure within a splat.

Figure 3 a) BSE image showing the etched HT coating cross section; and SE images showing b) the top surface, c) the equiaxed grain structure of the coating and d) the interface of the coating with the substrate.

Figure 4 Comparative graphs showing the obtained results of the COF and the δm (logarithmic scale) of the substrate and the as-sprayed and HT coatings.

Figure 5 SE, BSE and EDX microanalysis, acquired from the sites indicated in the BSE images, from the worn surfaces of the HT coating tested under unidirectional sliding conditions at RT (a, b and c) and at 450 °C (d, e and f), and under oscillating conditions at RT (g, h and i) and at 450 °C (j, k and l). The inserted micrographs in (b) and (e) are magnified images from the centre of those images.

Figure 6 BSE images (on the left) showing cross sections of worn HT coating samples and the corresponding Ti Kα, O K and Fe Kα EDX maps (on the right) from the squared detail of the cross section. The figures correspond to the samples tested under unidirectional sliding conditions at RT (a and b) and at 450 °C (c and d), and under oscillating movement at RT (e and f) and at 450 °C (g and h).

Figure 7 BF micrograph of a HT coating sample that have been tested at RT, applying a normal pressure of 30 MPa and an oscillation amplitude of 596 μm. A SADP and the EDX microanalysis acquired from the region indicated as R1 are included in the figure. Cu detection in the EDX analysis comes from the grid.

Figure 8 Annular dark-field (ADF) image and the Ti-Kα, Fe-Kα, Al-Kα, V-Kα, Cr-Kα, and Cr-Kβ STEM maps acquired from the area. The images were acquired from a HT coating sample tested at RT, applying a normal pressure of 30 MPa and an oscillation amplitude of 506 μm.

Figure 9 BF micrograph of the near surface of a HT coating sample tested at 450 °C, applying a normal pressure of 30 MPa and an oscillation amplitude of 596 μm. The EDX from the regions indicated by arrows are included. The EDX pattern on the right also showed peaks of Cu Kα, Cu Kβ and Pt Lα at higher energies. Pt was used for protecting the sample during the FIB preparation. Cu was the material of the grid where the FIB sample was stuck.

Figure 10 a) EELS spectrum acquired from the MML generated in the upper region of the sample presented in the above figure and magnifications of the regions related to the b) O-K and b) Fe-$L_{2,3}$ edges.

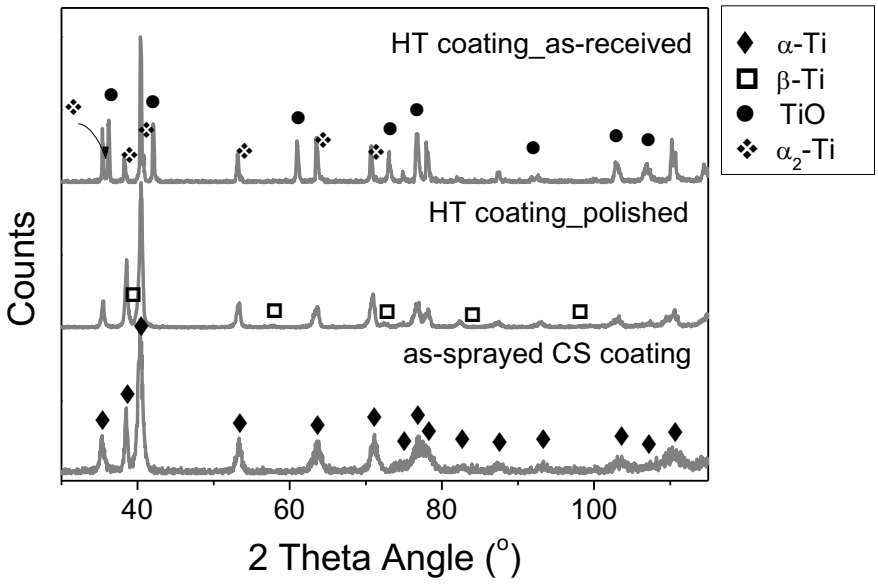

Figure 1

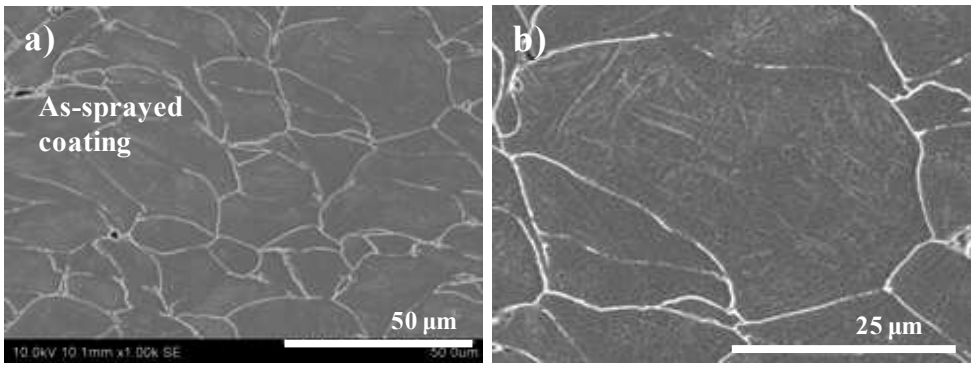

Figure 2

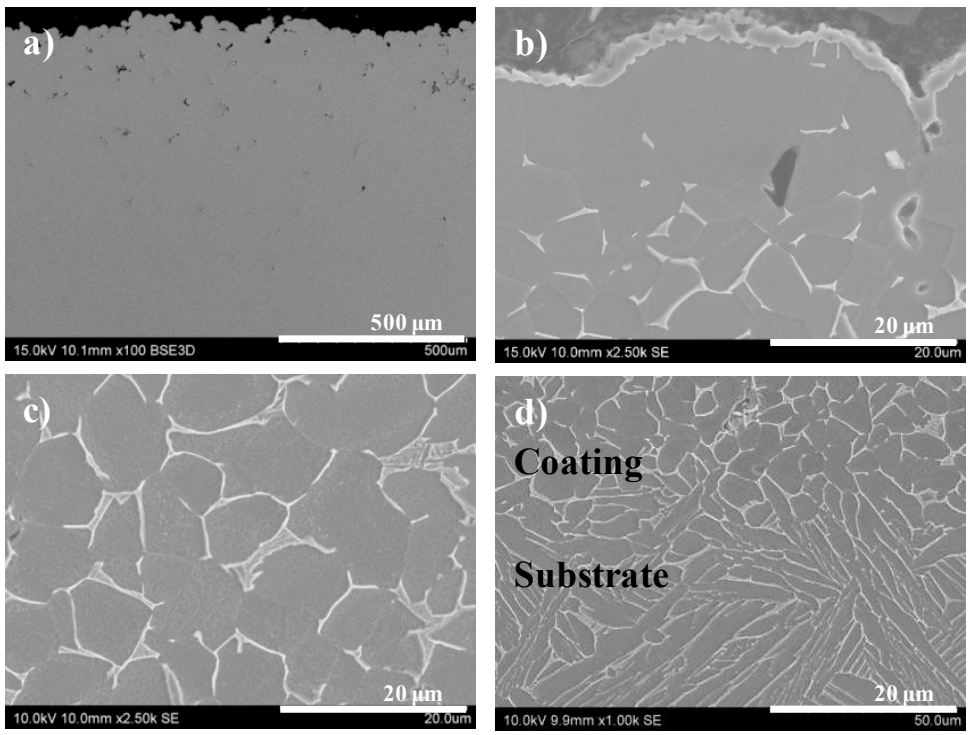

Figure 1

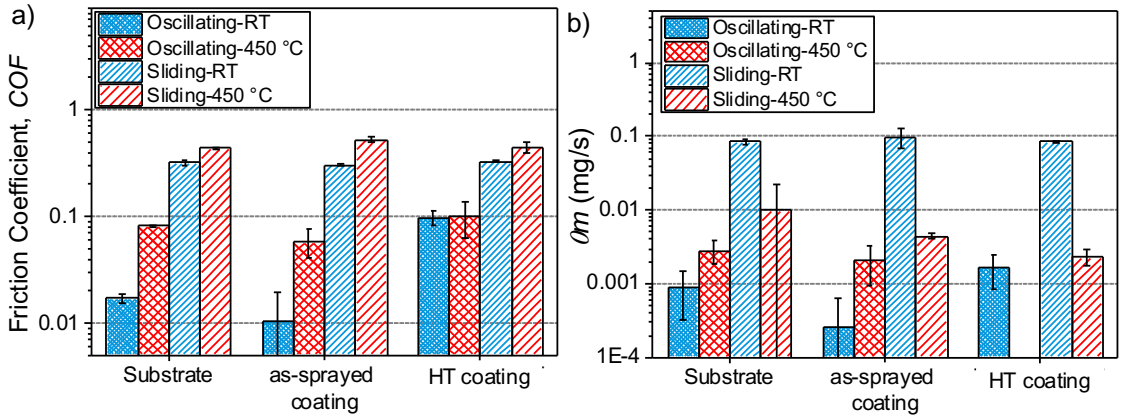

Figure 2

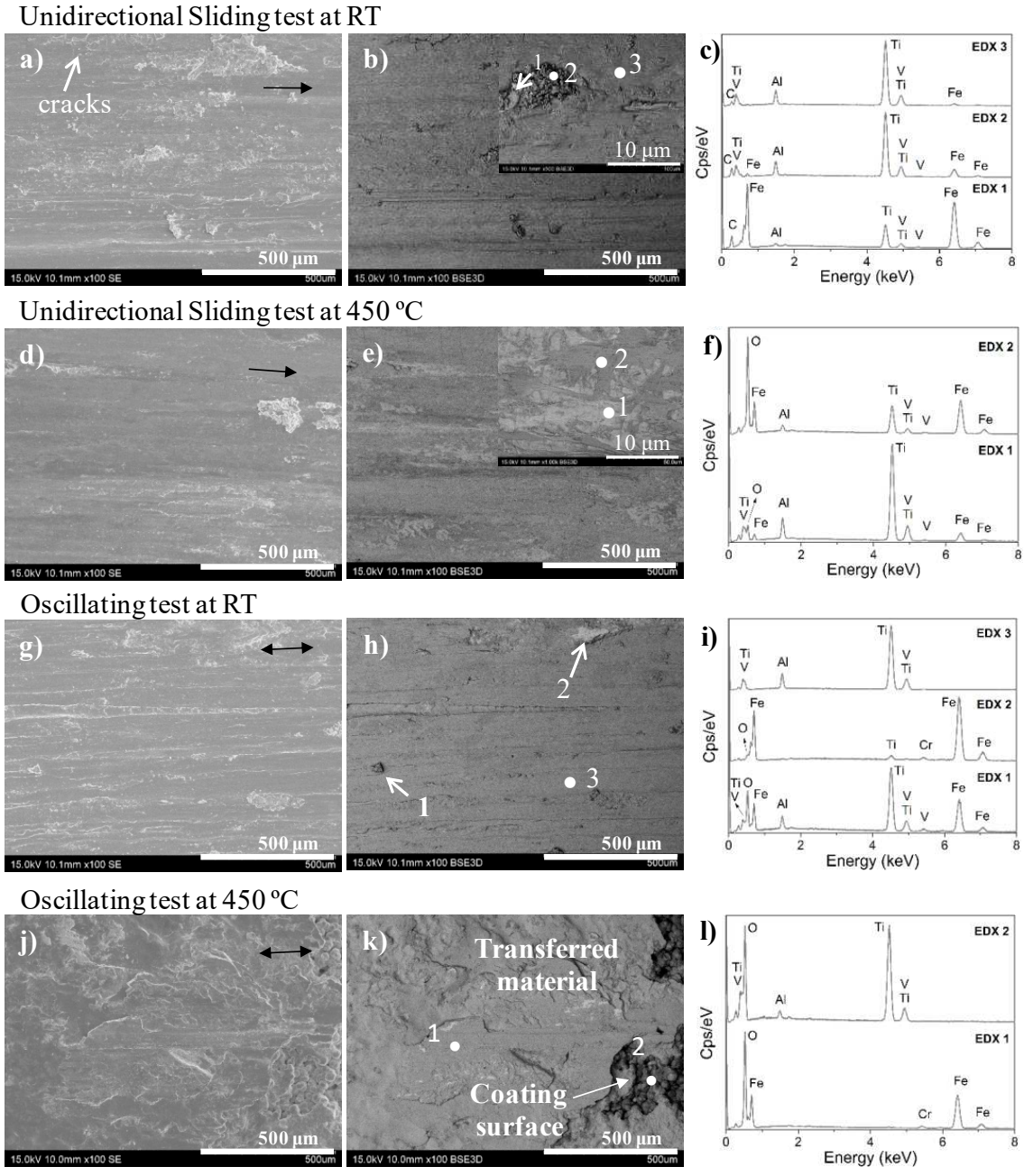

Figure 3

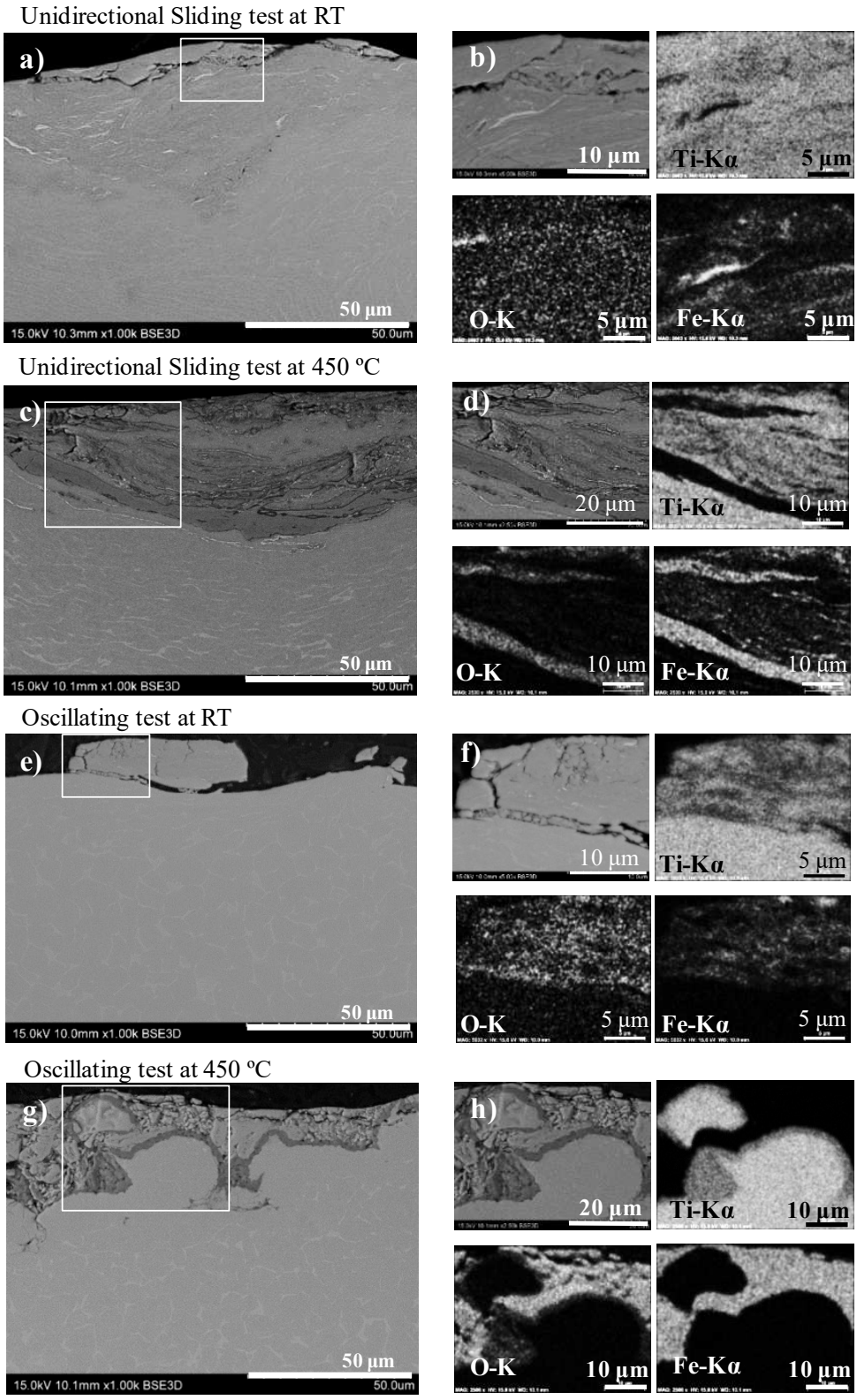
Unidirectional Sliding test at RT
a)
50 µm
15.0kV 10.3mm x1.00k BSE3D
50.0um
b)
10 µm
Ti-Kα
5 µm
O-K
5 µm
Fe-Kα
5 µm
Unidirectional Sliding test at 450 ºC
c)
50 µm
15.0kV 10.1mm x1.00k BSE3D
50.0um
d)
20 µm
Ti-Kα
10 µm
O-K
10 µm
Fe-Kα
10 µm
Oscillating test at RT
e)
50 µm
15.0kV 10.0mm x1.00k BSE3D
50.0um
f)
10 µm
Ti-Kα
5 µm
O-K
5 µm
Fe-Kα
5 µm
Oscillating test at 450 ºC
g)
50 µm
15.0kV 10.1mm x1.00k BSE3D
50.0um
h)
20 µm
Ti-Kα
10 µm
O-K
10 µm
Fe-Kα
10 µm

Figure 4

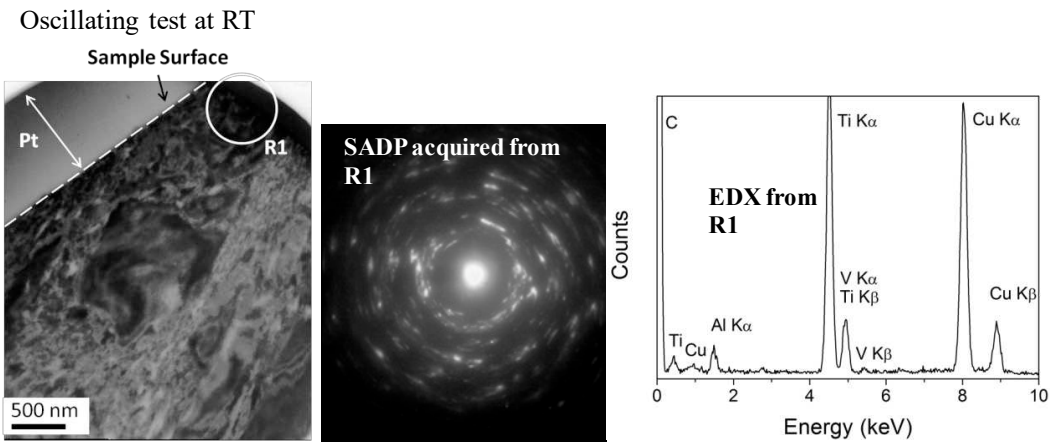

Figure 5

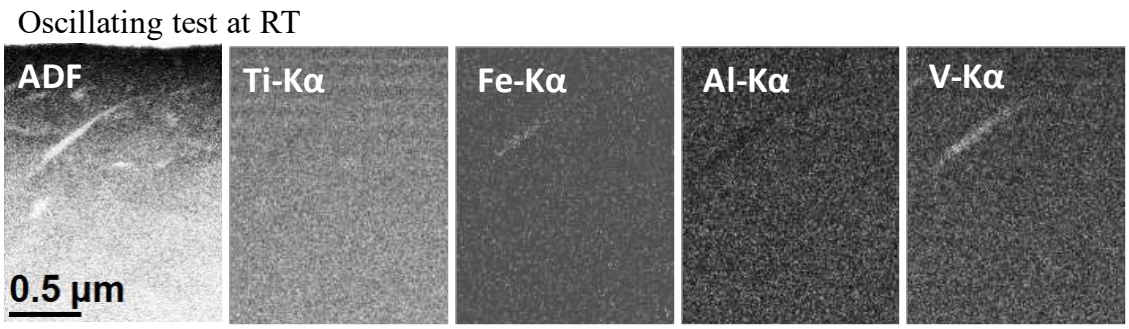

Figure 6

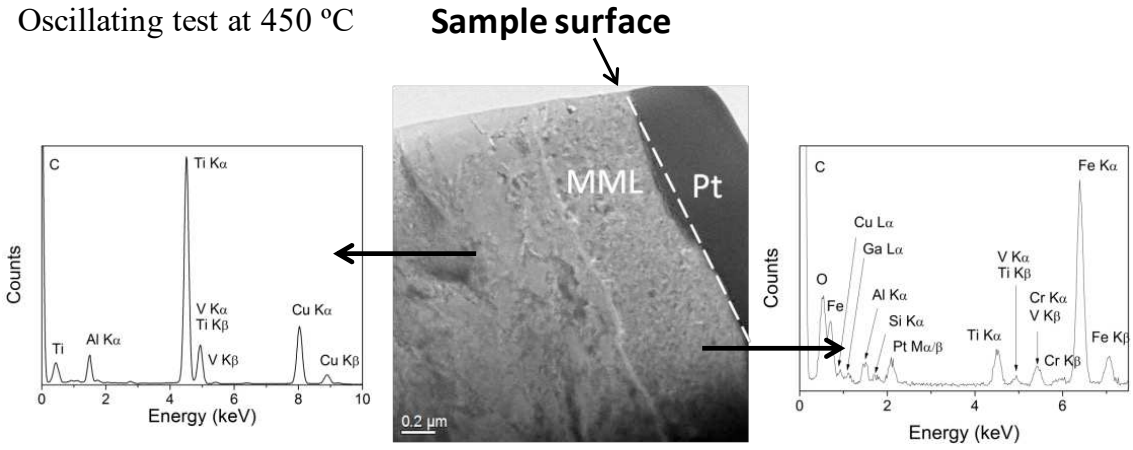

Figure 7

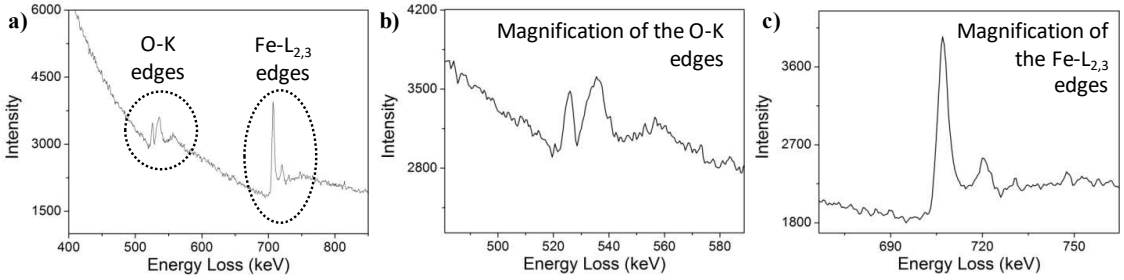

Figure 8